Journal of Robotics and Control (JRC)
Volume 6, Issue 2, 2025
ISSN: 2715-5072, DOI: 10.18196/jrc.v6i2.26073

A Comparative Study of Nonlinear Control and Passivity-Based Control using Neural Networks for A Bicycle Robot

Minh Ngoc Huynh [1], Hoai Nghia Duong [2*], Vinh Hao Nguyen [3]
[1, 3] Ho Chi Minh City University of Technology (HCMUT), Vietnam National University Ho Chi Minh City, Ho Chi Minh City, Vietnam
[2] Eastern International University, Binh Duong Province, Vietnam
[1] Industrial University of Ho Chi Minh City, Ho Chi Minh City, Vietnam
Email: [1] hmngoc.sdh20@hcmut.edu.vn, [2] nghia.duong@eiu.edu.vn, [3] vinhhao@hcmut.edu.vn
*Corresponding Author

***Abstract*—In this paper, a comparative study of nonlinear control and passivity-based control using neural networks for a bicycle robot is proposed. Bicycle robot is a nonlinear, multi-input multi-output system. Two inputs of a bicycle robot are the steering torque and kinetic energy. Its two outputs are the steering angle and the rolling angle. The control problem is that the steering angle and the rolling angle track a value of zero, and the velocity of the steering angle and velocity of the rolling angle track a value of zero to make a bicycle robot stabilize at its vertical balance. Firstly, an input-output linearization control law decouples the bicycle robot into single-input single-output systems. This plant is passive and zero-state observable. Secondly, the passivity-based control law is applied to each single-input single-output system. Finally, the neural network, which performs the passivity-based control, is applied to each single-input single-output system in order that the bicycle robot keeps its vertical balance. A training algorithm using the steepest descend method is proposed. The simulation results of the passivity-based control and the results of the passivity-based control using neural networks show that the bicycle robot keeps its vertical balance. The settling time of the steering angle and the rolling angle of the passivity-based control using a neural network, 1.8s, is shorter than that of the passivity-based control. There is a comparison with the passivity-based control combined with sliding mode control for a bicycle robot.**

***Keywords*—Bicycle Robot; Input-Output Linearization; Passivity-Based Control; Neural Network; Training Algorithm.**

I. INTRODUCTION

The bicycle robot is a nonlinear, multi-input, multi-output (MIMO) system that presents significant stability challenges. Due to its instability, controlling the bicycle robot to maintain vertical balance has been a subject of extensive research. The challenge of controlling the bicycle robot to remain balanced vertically has led to various approaches. For instance, [1] utilized the steering angle as the primary control input maintain vertical balance. Bicycle robot has the rolling angle as the output signal. In [2] presented the dynamical model of bicycle robot, input-output linearization, and feedback control using the pole placement. In [3] presented the dynamical model of bicycle robot and the exact linearization feedback control around the operating point. The sliding mode control and the passivity-based control of nonlinear systems were presented in [4]. Ref. [5] presented the Lyapunov stable theory, a passivation and the passivity-based control of a two-degree of freedom robot. The control of bicycle robot using input-output linearization was presented in [6]. The proportional derivative (PD) controller and the first-order compensator were applied to these single-input single-output systems. In [7] presented the passivity-based trajectory tracking control for autonomous bicycle. The passivity-based proportional integral (PI) control for bicycle robot was presented in [8]. Some control approaches were presented in [9]-[19]. In [9] described a combined control algorithm based on synchronous reinforcement learning to regulate a self-balancing bicycle robot. An learning-machine-based robust sliding mode control of bicycle robot was presented in [11]. In [13] presented the semi-empirical dynamics modeling of a bicycle robot based on feature selection and neural network. In [19] presented the mathematical model of the dynamic multi-rigid-body mechanical system of unmanned bicycle using the Kane method and the full state feedback control was described.

The passivation methods were presented in [20]-[22]. [20] described a passivation method of a plant using input-output matrix transformation. In Ref. [21] presented a passivation approach to the control design of non-passive nonlinear systems. Ref. [22] presented the cascade and passivity-based control designs for TORA example. The second order sliding mode control with disturbance observer was presented in [23] to stabilize the bicycle. In [24] presented the structure-mixed H_2/H_∞ control using the particle swarm optimization for the bicycle robot.

Some adaptive control and backstepping control approaches were presented in [25]-[34]. In [25] presented the passive backstepping control of dual active bridge converter in the modular three-port DC converter. In [29] presented the neural network integrated adaptive backstepping control of DC-DC boost converter. In [30] presented the combining of the passivity-based control and the quadratic regulator for a rotary inverted pendulum. A multikernel passive stochastic gradient algorithms and transfer learning was presented in [33]. In [34] presented an adaptive backstepping terminal sliding mode control which leverages a physics-informed neural network to control a DC-DC buck converter for a proton exchange membrane (PEM).

The passivity-based and its variations were presented in [35]-[45]. In [35] presented the passivity-based control, the sliding mode control and its applications to the electromechanical applications. In [36] presented a passivity-based control using genetic algorithm for a DC-DC boost power converter. In [37] presented the passivity-based control combined with sliding mode control for a DC-DC boost power converter. In [40] presented the passivity-based control of robots with theory and examples. In [45] presented the hybrid passivity-based control for stability and robustness enhancement in DC microgrid.

The neural network was presented in [46]-[56]. The fixed-time neural control for robot manipulator with global stability and guaranteed transient performance was presented in [46]. Ref. [47] presented the neural adaptive control of time-continuous systems. In [50] presented the passivity and passification of fuzzy memristive inertial neural networks on time scales. Ref. [52] presented an adaptive neural network control for narrowband active noise control systems. In [54] described the deep neural data-driven Koopman fractional control for a worm robot. In [55] presented the model predictive control using a varying parameter neural network for multi-robot tracking and formation. Some other neural control and robust control approaches were presented in [57]–[68]. A neural networks-based composite learning control for robotic systems [59]. A a robust two-stage active disturbance rejection control for the stabilization of a riderless bicycle [61]. A review on robust control of robot manipulators for future manufacturing was presented in [62]. In [63] presented the passivity-based swing-up control and sliding mode technique combined energy-based method for a rotary inverted pendulum. In [67] presented multilayer perceptron neural networks, modelling and control of dynamic systems. In [68] presented the holistic real-time model-based control for highly flexible robotic manufacturing cell.

Other control approaches for robot were presented in [69]-[78]. A passivity-based adaptive fuzzy control was presented in [69] for stochastic nonlinear switched systems via T-S fuzzy modeling. Ref. [70] presented the semipassivity-based fuzzy tracking control for switched nonlinear systems. In [73] presented the robotic arms for telemedicine system using smart sensors and ultrasound robots. The intelligent control with adaptive system for electrically assisted bicycle was presented in [75]. The cooperative control of electrical bicycles [76]. The simulation study of evaluating performance of shared autonomous bicycles [77]. Self-learning mechanism for the output regulation of second-order affine nonlinear systems [78].

In this paper, a comparative study of nonlinear control and passivity-based control using neural networks for a bicycle robot is proposed. A training algorithm is constructed. Simulation results are done with MATLAB/Simulink. Our control problem is that the steering angle and the rolling angle track a value of zero, and the velocity of steering angle and the velocity of rolling angle track a value of zero, and the control signals come to zero in order that the bicycle keeps its vertical balance.

The contribution is

- This paper applies input-output linearization to decouple the bicycle robot's dynamics into single- input, single-output (SISO) systems. Unlike previous studies, such as [8], which use passivity-based PI control, our method applies the passivity-based control law to these decoupled systems.
- Subsequently, we apply two the neural network-based controllers to the SISO systems. A novel training algorithm is proposed to optimize the passivity-based control using neural networks for improved stabilization of the bicycle robot. Then we compare with the passivity-based control combined with sliding mode control of [37] which is applied to a bicycle robot.

The remainder of the paper is organized as follows: Section 2 presents the dynamical model of a bicycle robot and explores its passivity-based properties. Section 3 discusses the proposed passivity-based control using neural networks, along with the training algorithm. The simulation results and discussions are presented in section 4. Finally, conclusions are presented in section 5.

II. Preliminary and Research Method

A. *Dynamical Model of a Bicycle Robot*

The parameters of a bicycle robot are described in Fig. 1 and Table I.

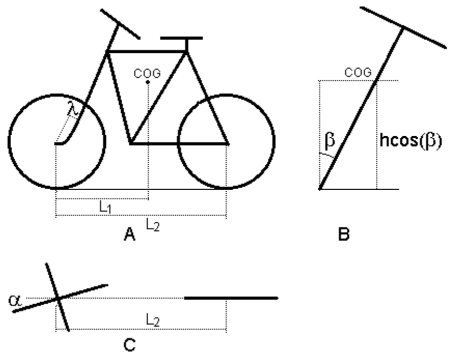

Fig. 1. The parameters of bicycle robot, A) side view; B) front view; C) top view

When the slipping of the wheels is omitted, the mathematical model of the bicycle robot in [2] is as follows

$$\begin{cases} \dot{x}_1 = x_2 \\ \dot{x}_2 = \dfrac{c_2 \sin(x_3)x_4^2 + c_3 u_1 + d_2 d_3 c_1 \tan(x_1)\cos^2(x_3)u_2}{1 - d_1 c_1 \cos^2(x_3)} \\ \dot{x}_3 = x_4 \\ \dot{x}_4 = \dfrac{0.5 d_1 c_2 \sin(2x_3)x_4^2 + d_1 c_3 \cos(x_3)u_1 + d_2 d_3 \tan(x_1)\cos(x_3)u_2}{1 - d_1 c_1 \cos^2(x_3)} \\ y_1 = x_1 \\ y_2 = x_3 \end{cases} \quad (1)$$

The bicycle robot is actuated by two motors. The first motor is placed at the axis of rear wheel so that the bicycle robot moves forward with the velocity, V. The second motor is placed at the axis of the steering device to control the steering angle.

TABLE I. THE PARAMETERS OF BICYCLE ROBOT

Name	Physical Meanings	Value
COG	Center of gravity	
m_1	Mass of each wheel	2.5 kg
m_2	Mass of the triangle frame	18 kg
r	Radius of the wheel	0.33 m
λ	Distance between the axis of the front fork and the front wheel	0.04 m
h	The height of COG	0.92 m
L_1	The distance between the projection of the axis of the front wheel and COG	0.7 m
L_2	The distance between the axis of the front wheel and the axis of the rear wheel	1.1 m
p	$(L_2-L_1)/L_2$	0.36
V	Forward moving velocity of bicycle	
α	The steering angle	
β	The rolling angle	

where $x_1 = \alpha,\ x_2 = \dot{\alpha},\ x_3 = \beta,\ x_4 = \dot{\beta}$. α is the steering angle. $\dot{\alpha}$ is the angle velocity of the steering angle.β is the rolling angle. $\dot{\beta}$ is the angle velocity of the rolling angle. $x = [x_1 \quad x_2 \quad x_3 \quad x_4]^T$. The outputs are the steering angle and the rolling angle. $y = [y_1 \quad y_2]^T$. The inputs are the steering torque of the second motor, u_1 (Nm) and the kinetic energy, u_2 (J). $u = [u_1 \quad u_2]^T$.

$$u_2 = \frac{(2m_1 + m_2)V^2}{2} \tag{2}$$

where

$c_1 = \frac{-(m_1 r + m_2 hp)\lambda}{m_1 r^2/2 + m_1\lambda^2 + m_2 p^2 \lambda^2}$,

$c_2 = \frac{(m_1 r + m_2 hp)\lambda}{m_1 r^2/2 + m_1\lambda^2 + m_2 p^2 \lambda^2}$,

$c_3 = \frac{1}{m_1 r^2/2 + m_1\lambda^2 + m_2 p^2 \lambda^2}$,

$d_1 = \frac{-(m_1 r + m_2 hp)\lambda}{3m_1 r^2 + 2m_2 h^2}$,

$d_2 = \frac{2(2m_1 r + m_2 h)}{(2m_1 + m_2)L_2}$,

$d_3 = \frac{1}{3m_1 r^2 + 2m_2 h^2}$

Our goal is to stabilize the bicycle at its vertical balance.

B. Passivity-based Property of Bicycle Robot

1) Input-Output Linearization of bicycle robot

From (1), we have

$$\begin{cases} \ddot{y}_1 = \dfrac{c_2 \sin(x_3) x_4^2 + c_3 u_1 + d_2 d_3 c_1 \tan(x_1)\cos^2(x_3) u_2}{1 - d_1 c_1 \cos^2(x_3)} \\ \ddot{y}_2 = \dfrac{0.5 d_1 c_2 \sin(2x_3) x_4^2 + d_1 c_3 \cos(x_3) u_1 + d_2 d_3 \tan(x_1)\cos(x_3) u_2}{1 - d_1 c_1 \cos^2(x_3)} \end{cases} \tag{3}$$

Or we have in the matrix form

$$\ddot{y} = f(x) + G(x)u \tag{4}$$

$$f(x) = \frac{c_2 x_4^2}{1 - d_1 c_1 \cos^2(x_3)} \begin{bmatrix} \sin(x_3) \\ 0.5 d_1 \sin(2x_3) \end{bmatrix} \tag{5}$$

$$G(x) = \frac{1}{1 - d_1 c_1 \cos^2(x_3)} \times \begin{bmatrix} c_3 & d_2 d_3 c_1 \tan(x_1)\cos^2(x_3) \\ d_1 c_3 \cos(x_3) & d_2 d_3 \tan(x_1)\cos(x_3) \end{bmatrix} \tag{6}$$

with condition: $1 - d_1 c_1 \cos^2(x_3) \neq 0$.

From (4), input – output linearization control law is as (7).

$$\ddot{y} = v \tag{7}$$

v is a control variable of (7).

From (4) and (7), the control law u is

$$u = G(x)^{-1}[v - f(x)] \tag{8}$$

$$u = \begin{bmatrix} \dfrac{1}{c_3} & \dfrac{-c_1 \cos(x_3)}{c_3} \\ \dfrac{-d_1}{d_2 d_3 \tan(x_1)} & \dfrac{1}{d_2 d_3 \cos(x_3)\tan(x_1)} \end{bmatrix} [v - f(x)] \tag{9}$$

with condition:$\tan(x_1) \neq 0$.

Eq. (7) can be presented for each SISO system

$$\ddot{y} = v \Rightarrow \begin{bmatrix} \ddot{y}_1 \\ \ddot{y}_2 \end{bmatrix} = \begin{bmatrix} v_1 \\ v_2 \end{bmatrix} \tag{10}$$

Or we rewrite as follows

$$\ddot{y}_1 = v_1 \tag{11}$$

$$\ddot{y}_2 = v_2 \tag{12}$$

2) Passivity-based Property of bicycle robot

Eq. (7) is rewritten as follows

$$\begin{aligned} \dot{z}_1 &= z_2 \\ \dot{z}_2 &= v \\ h &= z_2 \end{aligned} \tag{13}$$

We choose the storage function $V_a V_1$ as follows

$$V_a = \frac{1}{2}x_2^2 + \frac{1}{2}x_4^2 \tag{14}$$

V_a is positive definite.

The derivative of V_a is as follows

$$\dot{V}_a = x_2\dot{x}_2 + x_4\dot{x}_4 \tag{15}$$

We have

$$\dot{y}^T v = \dot{y}_1 v_1 + \dot{y}_2 v_2 = x_2\dot{x}_2 + x_4\dot{x}_4 = \dot{V}_a \tag{16}$$

The plant (7), which has the input v and the output $\dot{y}$, is passive because of $\dot{y}^T v \geq \dot{V}_a$

The plant (7) is zero-state observable because $v = 0, z_2 = \dot{y} = \begin{bmatrix} x_2 \\ x_4 \end{bmatrix} = \begin{bmatrix} 0 \\ 0 \end{bmatrix} \Rightarrow \dot{x}_2 = 0, \dot{x}_4 = 0 z_1 = \begin{bmatrix} x_1 \\ x_3 \end{bmatrix} = \begin{bmatrix} 0 \\ 0 \end{bmatrix}$

The plant (7) is separated into two SISO systems. The passivity-based control law is applied to each SISO system.

According to (7) and the property [5], the passivity-based control law for each SISO system is as (17).

$$v = -\phi(\dot{y}) \text{ with } \phi(0) = 0; \dot{y}^T\phi(\dot{y}) > 0\forall\dot{y} \neq 0$$
$$\phi(\dot{y}) = a_1\dot{y} + a_3\dot{y}^3 + a_5\dot{y}^5 \quad (17)$$
$$v_1 = -\phi_1(\dot{y}_1) \text{ with } \phi_1(0) = 0; \dot{y}_1\phi_1(\dot{y}_1) > 0\forall\dot{y}_1 \neq 0$$

We can choose

$$\phi_1(\dot{y}_1) = a_1\dot{y}_1 + a_3\dot{y}_1^3 + a_5\dot{y}_1^5 \quad (18)$$

$$v_1 = -a_1\dot{y}_1 - a_3\dot{y}_1^3 - a_5\dot{y}_1^5 \quad (19)$$

$$v_2 = -\phi_2(\dot{y}_2) \text{ with } \phi_2(0) = 0; \dot{y}_2\phi_2(\dot{y}_2) > 0\forall\dot{y}_2 \neq 0 \quad (20)$$

We can choose

$$\phi_2(\dot{y}_2) = a_1\dot{y}_2 + a_3\dot{y}_2^3 + a_5\dot{y}_2^5 \quad (21)$$

$$v_2 = -a_1\dot{y}_2 - a_3\dot{y}_2^3 - a_5\dot{y}_2^5 \quad (22)$$

We have

$$\dot{V}_a \leq \dot{y}^T v \Rightarrow \dot{V}_a \leq -\dot{y}^T\phi(\dot{y}) \leq 0\forall\dot{y} \neq 0$$

So $\dot{V}_a$ is negative semidefinite.

The passivity-based control diagram for bicycle robot is described in Fig. 2.

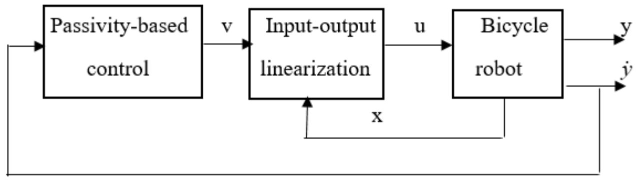

Fig. 2. The structure of the passivity-based control for bicycle robot

III. The Passivity-based Control using Neural Networks

A. *Passivity-based Control using Neural Networks*

The structure of the Adaline neural network is illustrated in Fig. 3.

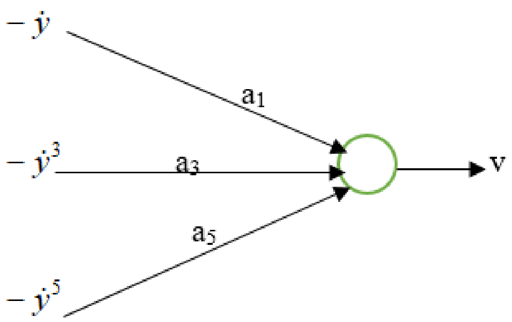

Fig. 3. The structure of the Adaline neural network

The neural network control diagram is described in Fig. 4.

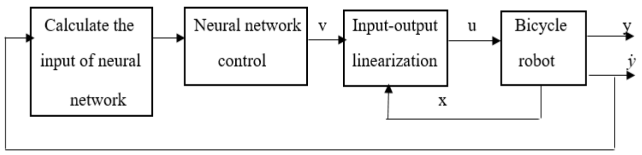

Fig. 4. The diagram of the neural network control

Now we construct the neural networks which perform the passivity-based control law (19), (22). We use two neural networks. The first neural network performs the control law (19). The neural network has two layers. The input layer has three inputs: $-\dot{y}_1$, $-\dot{y}_1^3$, $-\dot{y}_1^5$. The output layer has one outputs v_1 and its activation function is linear. The second neural network performs the control law (22). The neural network has two layers. The input layer has three inputs: $-\dot{y}_2$, $-\dot{y}_2^3$, $-\dot{y}_2^5$. The output layer has one outputs v_2 and its activation function is linear. The weights a_1, a_2, and a_3 of the neural network are adjusted in the online manner.

B. *A Training Algorithm of Neural Network*

A training algorithm is as follows:

Eq. (13) is rewritten as (23).

$$\dot{z} = f(z) + g(z)v$$
$$h = z_2 \quad (23)$$

Where

$$f(z) = \begin{bmatrix} z_2 \\ 0 \end{bmatrix} \quad (24)$$

$$g(z) = \begin{bmatrix} 0 \\ 1 \end{bmatrix} \quad (25)$$

The plant (7) is passive and zero-state observable. According to (17) and (20), we have,

$$v = -\phi(\dot{y}) \text{ with } \phi(0) = 0; \dot{y}\phi(\dot{y}) > 0\forall\dot{y} \neq 0$$

We can choose,

$$\phi(\dot{y}) = \sum_{i=1}^{m} a_{2i-1}\dot{y}^{2i-1} \quad (26)$$

The passivity-based control law v is (27)

$$v = -\sum_{i=1}^{m} a_{2i-1}\dot{y}^{2i-1} = -\Phi^T\theta \quad (27)$$

Where

$$\Phi = [\dot{y} \quad \dot{y}^3 \quad \dot{y}^5 \quad \dots \quad \dot{y}^{2m-1}]^T \text{ and}$$
$$\theta = [a_1 \quad a_3 \quad a_5 \quad \dots \quad a_{2m-1}] \quad (28)$$

The performance criterion is (29).

$$J = \frac{q}{2}\dot{y}^2 + \frac{r_1}{2}v^2 \quad (29)$$

Where $q \geq 0; r_1 \geq 0$. Using the steepest descend method,

$$\theta(k+1) = \theta(k) - \eta\left(\frac{\partial J}{\partial \theta}\right)^T \quad (30)$$

Where $\eta > 0$ is the learning constant and,

$$\frac{\partial J}{\partial \theta} = \left[\frac{\partial J}{\partial a_1} \quad \frac{\partial J}{\partial a_3} \quad \frac{\partial J}{\partial a_5} \quad \dots \quad \frac{\partial J}{\partial a_{2m-1}}\right] \quad (31)$$

We have

$$\frac{\partial J}{\partial \theta} = \frac{\partial J}{\partial \dot{y}}\frac{\partial \dot{y}}{\partial z}\frac{\partial z}{\partial \theta} + \frac{\partial J}{\partial v}\frac{dv}{d\theta} = q\dot{y}\frac{\partial h}{\partial z}\frac{dz}{d\theta} + r_1 v\frac{dv}{d\theta} \quad (32)$$

The operating point of the plant (33).

$$f(z) + g(z)v = 0 \tag{33}$$

Taking the derivative of (33) with respect to θ yields

$$\frac{\partial f}{\partial z}\frac{dz}{d\theta} + \frac{\partial g}{\partial z}\frac{dz}{d\theta}v + g\frac{dv}{d\theta} = 0 \tag{34}$$

$$\Rightarrow \left(\frac{\partial f}{\partial z} + \frac{\partial g}{\partial z}v\right)\frac{dz}{d\theta} = -g\frac{dv}{d\theta} \tag{35}$$

$$\Rightarrow \frac{dz}{d\theta} = -\left(\frac{\partial f}{\partial z} + \frac{\partial g}{\partial z}v\right)^{-1} g\frac{dv}{d\theta} \tag{36}$$

Insert (36) into (32) yields

$$\frac{dJ}{d\theta} = \left(-q\dot{y}\frac{\partial h}{\partial z}\left(\frac{\partial f}{\partial z} + \frac{\partial g}{\partial z}v\right)^{-1} g + r_1 v\right)\frac{dv}{d\theta} \tag{37}$$

Where

$$\frac{dv}{d\theta} = \left[\frac{dv}{da_1} \quad \frac{dv}{da_3} \quad \frac{dv}{da_5} \quad \cdots \quad \frac{dv}{da_{2m-1}}\right] \tag{38}$$

Taking derivative of (27) with respect to a_k yields

$$\frac{dv}{da_k} = -\dot{y}^k - \sum_{k=1}^{m}(2i-1)a_{2i-1}\dot{y}^{2i-2}\frac{d\dot{y}}{da_k} \tag{39}$$

For k=1, 3, 5, …, 2m-1. Thus

$$\begin{aligned}\frac{dv}{d\theta} = [&-\dot{y} - \sum_{k=1}^{m}(2i-1)a_{2i-1}\dot{y}^{2i-2}\frac{d\dot{y}}{da_1},\\ &-\dot{y}^3 - \sum_{k=1}^{m}(2i-1)a_{2i-1}\dot{y}^{2i-2}\frac{d\dot{y}}{da_3},\\ &-\dot{y}^5 - \sum_{k=1}^{m}(2i-1)a_{2i-1}\dot{y}^{2i-2}\frac{d\dot{y}}{da_5},\dots,\\ &-\dot{y}^{2m-1} - \sum_{k=1}^{m}(2i-1)a_{2i-1}\dot{y}^{2i-2}\frac{d\dot{y}}{da_{2m-1}}]\\ = &-\Phi^T - \sum_{k=1}^{m}(2i-1)a_{2i-1}\dot{y}^{2i-2}\frac{d\dot{y}}{d\theta}\end{aligned} \tag{40}$$

On the other hand

$$\frac{d\dot{y}}{d\theta} = \frac{\partial h}{\partial z}\frac{dz}{d\theta} \tag{41}$$

Insert (36) into (41) yields

$$\frac{d\dot{y}}{d\theta} = -\frac{\partial h}{\partial z}\left(\frac{\partial f}{\partial z} + \frac{\partial g}{\partial z}v\right)^{-1} g\frac{dv}{d\theta} \tag{42}$$

Insert (42) into (40) yields

$$\frac{dv}{d\theta} = -\Phi^T + \sum_{k=1}^{m}(2i-1)a_{2i-1}\dot{y}^{2i-2}\frac{\partial h}{\partial z}\left(\frac{\partial f}{\partial z} + \frac{\partial g}{\partial z}v\right)^{-1} g\frac{dv}{d\theta} \tag{43}$$

$$\left(1 - \sum_{k=1}^{m}(2i-1)a_{2i-1}\dot{y}^{2i-2}\frac{\partial h}{\partial z}\left(\frac{\partial f}{\partial z} + \frac{\partial g}{\partial z}v\right)^{-1} g\right)\frac{dv}{d\theta} = -\Phi^T \tag{44}$$

$$\Rightarrow \frac{dv}{d\theta} = \frac{-\Phi^T}{1 - \sum_{k=1}^{m}(2i-1)a_{2i-1}\dot{y}^{2i-2}\frac{\partial h}{\partial z}\left(\frac{\partial f}{\partial z} + \frac{\partial g}{\partial z}v\right)^{-1} g} \tag{45}$$

Insert (45) into (37) yields

$$\frac{dJ}{d\theta} = \frac{-\left(-q\dot{y}\frac{\partial h}{\partial z}\left(\frac{\partial f}{\partial z} + \frac{\partial g}{\partial z}v\right)^{-1} g + r_1 v\right)\Phi^T}{1 - \sum_{k=1}^{m}(2i-1)a_{2i-1}\dot{y}^{2i-2}\frac{\partial h}{\partial z}\left(\frac{\partial f}{\partial z} + \frac{\partial g}{\partial z}v\right)^{-1} g} \tag{46}$$

The training algorithm is obtained by inserting (46) into (30).

$$\theta(k+1) = \theta(k) + \frac{\eta\left(-q\dot{y}\frac{\partial h}{\partial z}\left(\frac{\partial f}{\partial z} + \frac{\partial g}{\partial z}v\right)^{-1} g + r_1 v\right)\Phi}{1 - \sum_{k=1}^{m}(2i-1)a_{2i-1}\dot{y}^{2i-2}\frac{\partial h}{\partial z}\left(\frac{\partial f}{\partial z} + \frac{\partial g}{\partial z}v\right)^{-1} g} \tag{47}$$

q influences $\dot{y}$ and r_1 influences v.

Note that if we choose m=3, q=1, r_1=1, then we obtain

$$\frac{\partial f}{\partial z} = \begin{bmatrix}0 & 1\\0 & 0\end{bmatrix}; \frac{\partial g}{\partial z} = \begin{bmatrix}0 & 0\\0 & 0\end{bmatrix}$$

$$\left(\frac{\partial f}{\partial z} + \frac{\partial g}{\partial z}v\right)^{-1} = \begin{bmatrix}0 & 1\\0 & 0\end{bmatrix}$$

$$\frac{\partial h}{\partial z}\left(\frac{\partial f}{\partial z} + \frac{\partial g}{\partial z}v\right)^{-1} = [0 \quad 0]$$

$$\frac{\partial h}{\partial z}\left(\frac{\partial f}{\partial z} + \frac{\partial g}{\partial z}v\right)^{-1} g = 0$$

Then

$$\theta(k+1) = \theta(k) + \eta r_1 v\Phi$$

$$\dot{\theta} = \frac{\theta(k+1) - \theta(k)}{T} = \frac{\eta r_1 v\Phi}{T} \tag{48}$$

Now $\theta = [a_1 \quad a_3 \quad a_5]$, $\Phi = [\dot{y} \quad \dot{y}^3 \quad \dot{y}^5]^T$. T is a sample time. In this paper, the authors want to choose q=1, r_1=1. θ is the parameters of the passivity-based control which is optimized by the training algorithm.

C. *Comparison with Passivity-based Control combined with Sliding Mode Control*

We compare the passivity-based control using a neural network (PBC-NC) and the passivity-based control combined with sliding mode control (PBC-SMC) of [37] which is applied to the bicycle robot. The control law is as follows

$$v_{PBC-SMC} = -a_1\dot{y} - a_3\dot{y}^3 - a_5\dot{y}^5 - Ksign(\dot{y}) \tag{49}$$

$$v_{1PBC-SMC} = -a_1\dot{y}_1 - a_3\dot{y}_1^3 - a_5\dot{y}_1^5 - k_1 sign(\dot{y}_1) \tag{50}$$

$$v_{2PBC-SMC} = -a_1\dot{y}_2 - a_3\dot{y}_2^3 - a_5\dot{y}_2^5 - k_2 sign(\dot{y}_2) \tag{51}$$

K is a positive definite matrix. $k_1 > 0$, $k_2 > 0$

IV. SIMULATION AND DISCUSSION

The system is described in (1). Replace the value in Table I, we obtain: c_1=1.90, c_2=1.90, c_3=6.95, d_1=-0.0088, d_2=1.44, d_3=0.032, d_4=0.582. Choose q=1, r_1=1, $\eta = 0.001$. Initially, x_{10}=0.01, x_{20}=-0.01, x_{30}=0.01, x_{40}=-0.02, a_1=2, a_3=1.5, a_5=1.5, k_1=4, k_2=4. The simulation time is 10 s. T=0.001 s.

A. Passivity-based Control

Fig. 5 shows the angle velocity of the steering angle and the angle velocity of the rolling angle. Fig. 6 shows the output signals y_1, y_2 and the control signals u_1, $u_2$of the passivity-based control for bicycle robot.

The angle velocity of the steering angle $\dot{\alpha}$ and the angle velocity of the rolling angle $\dot{\beta}$ come to 0 (rad/s) and the settling time, t_s, is 2.4 s. The output y_1 is equal to 0.005 (rad) and t_s is 2 s. The output y_2 is equal to 0 (rad) and t_s is 2 s. The control signal $u_1$and the control signal $u_2$are equal to 0, and the settling time is 2 s. The bicycle robot is stabilized at the balance position vertically.

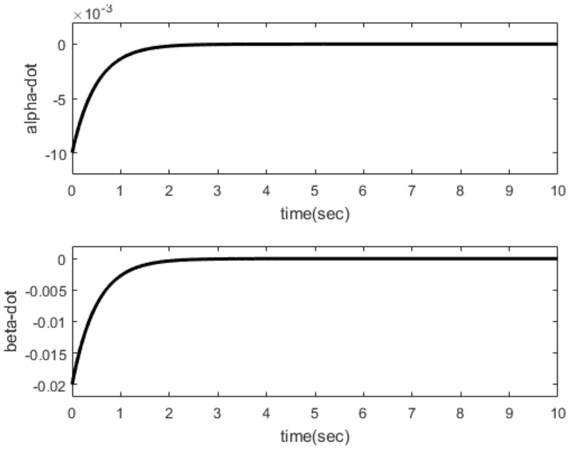

Fig. 5. The PBC results for bicycle robot: the angle velocity of the steering angle and the angle velocity of the rolling angle

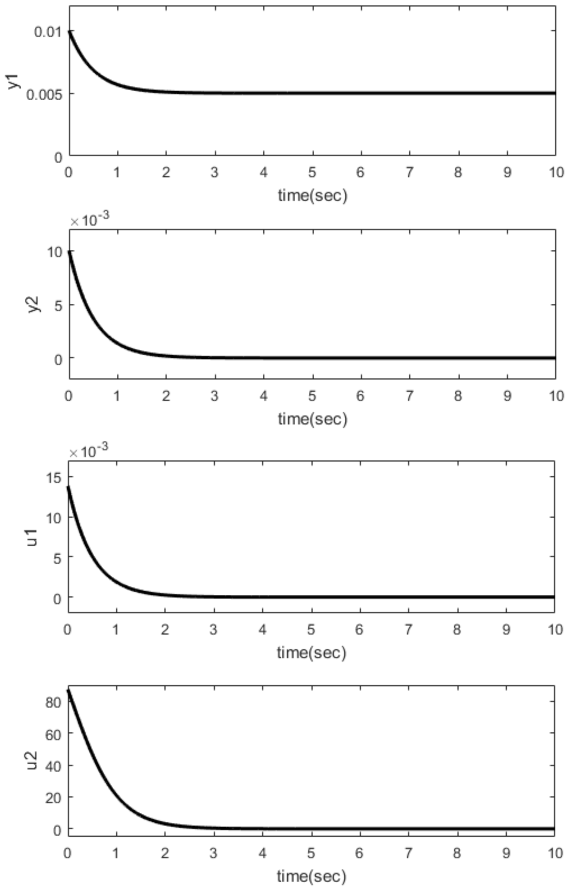

Fig. 6. The PBC results for bicycle robot: the output signals y_1, y_2 and the control signal u_1, u_2

B. Passivity-based Control using Neural Networks

Fig. 7 shows the angle velocity of the steering angle and the angle velocity of the rolling angle. Fig. 8 shows the output signals y_1, y_2 and the control signals u_1, $u_2$of the passivity-based control using a neural network (PBC-NC) for bicycle robot.

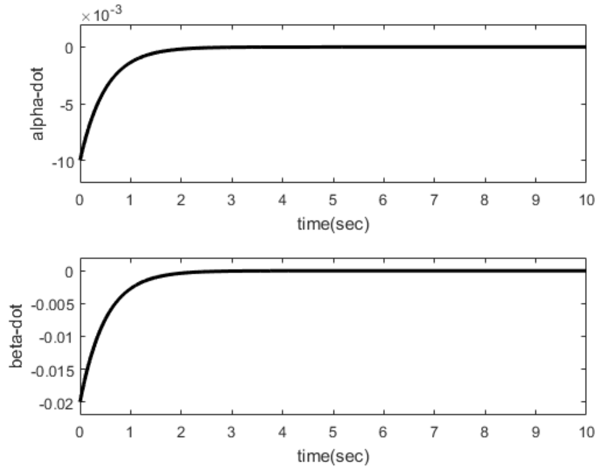

Fig. 7. The PBC-NC results for bicycle robot: the angle velocity of the steering angle and the angle velocity of the rolling angle

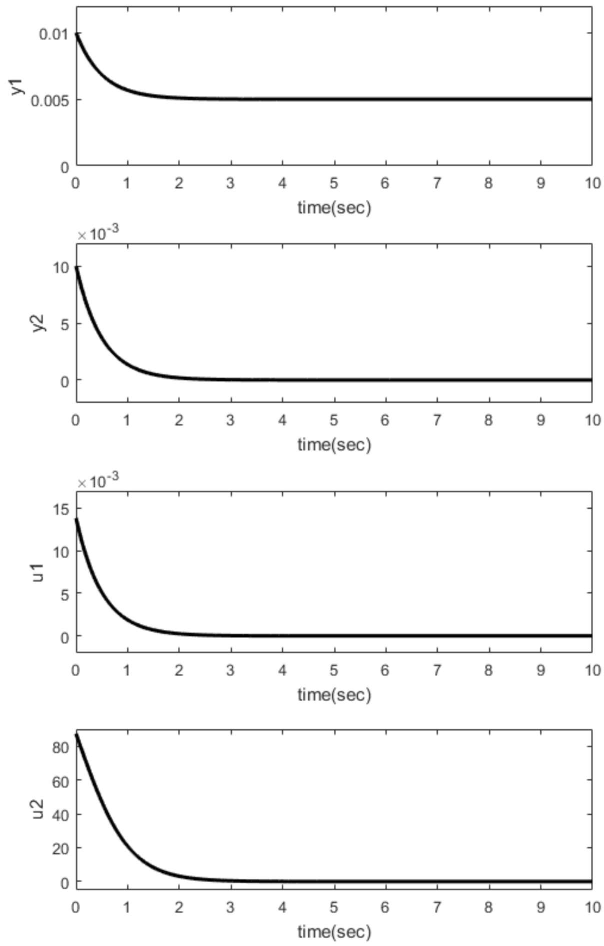

Fig. 8. The PBC-NC results for bicycle robot: the output signals y_1, y_2 and the control signal u_1, u_2

The angle velocity of the steering angle $\dot{\alpha}$ and the angle velocity of the rolling angle $\dot{\beta}$ come to 0 (rad/s) and the settling time, t_s, is 2.3 s. The output $y_1$is equal to 0.005 (rad) and the settling time is 1.8 s. The output y_2 is equal to 0 (rad) and the settling time is 1.8 s. The control signal u_1 is equal to 0 and t_s is 1.9 s. The control signal u_2 is equal to 0 and t_s is 2 s. Simulation results of the passivity-based control using neural network show that the bicycle robot is stabilized at the balance position vertically.

We compare the passivity-based control and the passivity-based control using a neural network. The comparison results are described in Table II.

TABLE II. THE RESULTS OF THE PBC-NC, PBC, AND PBC-SMC FOR BICYCLE ROBOT

Controller	α and β		$\dot{\alpha}$ and $\dot{\beta}$	
	Error	t_s (s)	Error	t_s (s)
PBC-NC with η=0.001	$\alpha \rightarrow$ 0.005 and $\beta \rightarrow 0$	1.8	$\dot{\alpha} \rightarrow 0$ and $\dot{\beta} \rightarrow 0$	2.3
PBC	$\alpha \rightarrow$ 0.005 and $\beta \rightarrow 0$	2	$\dot{\alpha} \rightarrow 0$ and $\dot{\beta} \rightarrow 0$	2.4
PBC-SMC of [37] applied to bicycle robot	$\alpha \rightarrow$ 0.011585 and $\beta \rightarrow$ 0.005	1.5	$\dot{\alpha} \rightarrow 0$ and $\dot{\beta} \rightarrow 0$	1.5

The passivity-based control using a neural network (PBC-NC), with η =0.001, demonstrates a shorter settling time for both the steering angle and rolling angle when compared to the traditional passivity-based control (PBC). The settling times of $\dot{\alpha}$ and the $\dot{\beta}$ of the PBC-NC, 2.3s, are shorter than that of the PBC, 2.4s.

We compare the PBC-NC with η =0.001 and the PBC-SMC of [37] which is applied to the bicycle robot. The comparison results are described in Table II.

Fig. 9 shows the angle velocity of the steering angle and the angle velocity of the rolling angle. Fig. 10 shows the output signals y_1, y_2 and the control signals u_1, u_2 of the passivity-based control combined with sliding mode control (PBC-SMC) for bicycle robot.

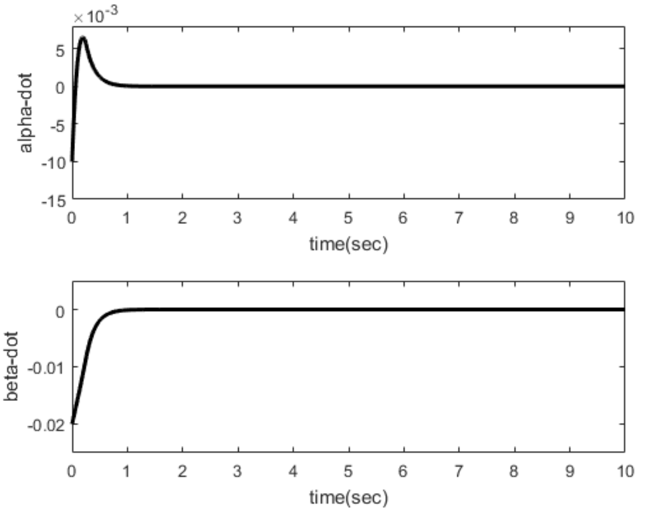

Fig. 9. The PBC-SMC results for bicycle robot: the angle velocity of the steering angle and the angle velocity of the rolling angle

The angle velocity of the steering angle $\dot{\alpha}$ and the angle velocity of the rolling angle $\dot{\beta}$ come to 0 (rad/s) and the settling time, t_s, is 1.5 s. The output y_1 is equal to 0.011585 (rad) and t_s is 1.5 s. The output y_2 is equal to 0.005 (rad) and t_s is 1.5 s. The control signal u_1 and the control signal u_2 are equal to 0 and t_s is 1.8 s. The bicycle robot is stabilized at the balance position vertically. We can see that the PBC-SMC has shorter settling time than the PBC-NC. However, the output y_2 of PBC-SMC is equal to 0.005 and the output y_2 of PBC-NC is equal to 0.

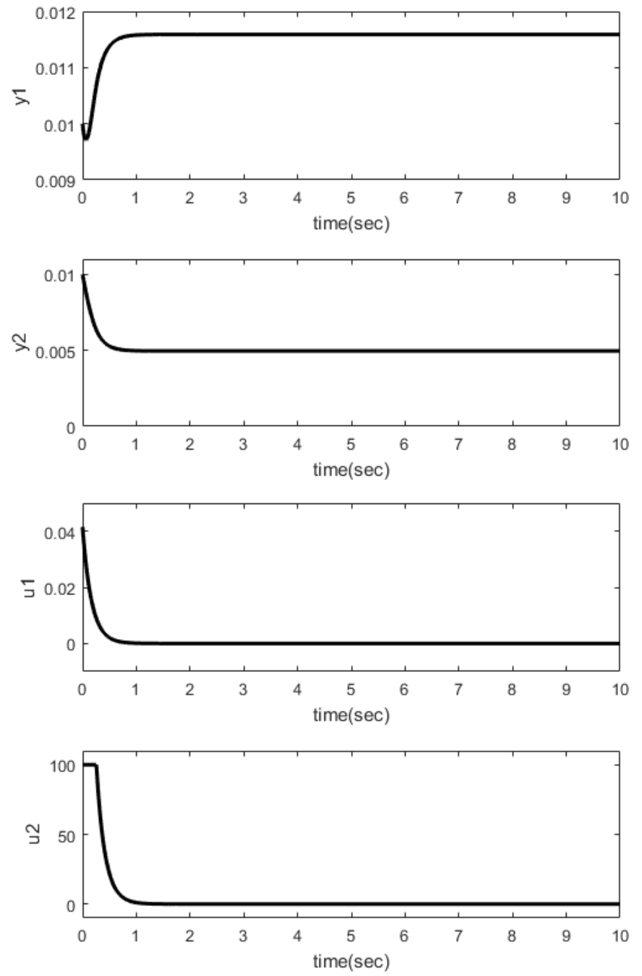

Fig. 10. The PBC-SMC results for bicycle robot: the output signals y_1, y_2 and the control signal u_1, u_2

We define the tracking error

$$e = y - y_d = \begin{bmatrix}\alpha\\ \beta\end{bmatrix} - \begin{bmatrix}0\\ 0\end{bmatrix} = \begin{bmatrix}\alpha\\ \beta\end{bmatrix}; \dot{e} = \begin{bmatrix}\dot{\alpha}\\ \dot{\beta}\end{bmatrix}$$

Where y_d = [0; 0]. The goal is that the steering angle tracks to zero and the rolling angle tracks to zero, the $\dot{\alpha}$ and $\dot{\beta}$ track to zero, and the control signals u_1 and u_2 come to zero.

The Fig. 11 shows the error of steering angle of the PBC-NC and the PBC. The Fig. 12 shows the error of rolling angle of the PBC-NC and the PBC. The results show that the error of steering angle of the PBC-NC and the PBC comes to 0.005 (rad), and the settling time of the PBC-NC, 1.8s is shorter than that of the PBC, 2 s. The results show that the error of rolling angle of the PBC-NC and the PBC comes to 0. The settling time of the PBC-NC, 1.8s is shorter than that of the PBC, 2s.

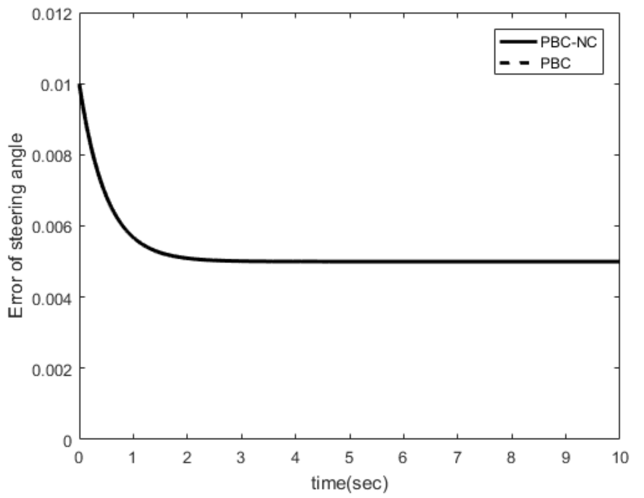

Fig. 11. The error of steering angle of the PBC-NC and the PBC for bicycle robot

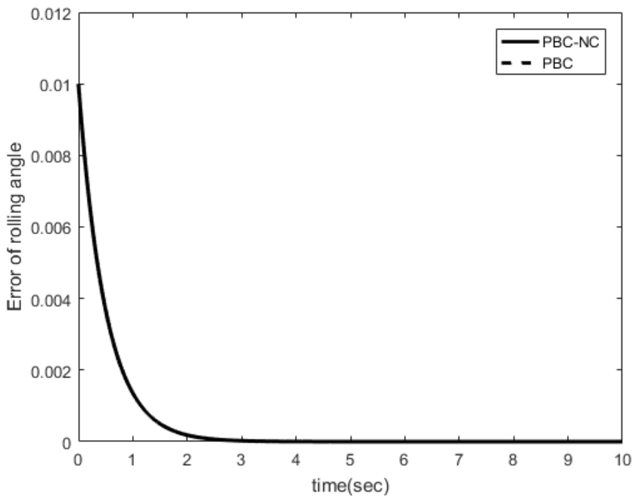

Fig. 12. The error of rolling angle of the PBC-NC and the PBC for bicycle robot

Let the learning constant, η, be 0.1. Fig. 13 shows the angle velocity of the steering angle and the angle velocity of the rolling angle of the PBC-NC when η is increased to 0.1. Fig. 14 shows the output signals y_1, y_2 and the control signals u_1, u_2 of the passivity-based control using neural network for bicycle robot when η is increased to 0.1.

The angle velocity of the steering angle $\dot{\alpha}$ comes to 0 at the settling time, t_s, 1.6 s. The angle velocity of the rolling angle $\dot{\beta}$ comes to 0 (rad/s) and the settling time, t_s is 1.6 s. The output y_1 is equal to 0.005 (rad) and t_s is 1.5 s. The output y_2 is equal to 0 (rad) and t_s is 1.5 s. The control signal u_1 and the control signal u_2 are equal to 0 and the settling time is 1.5 s. Simulation results of the passivity-based control using neural networks show that the bicycle robot is stabilized at the balance position vertically.

The results show that the settling time of the α and the β of the passivity-based control using neural networks (PBC-NC) is shorter than that of the PBC when η is increased to 0.1. The results show that the settling time of the $\dot{\alpha}$ and the $\dot{\beta}$ of the PBC-NC is shorter than that of the PBC when η is increased to 0.1.

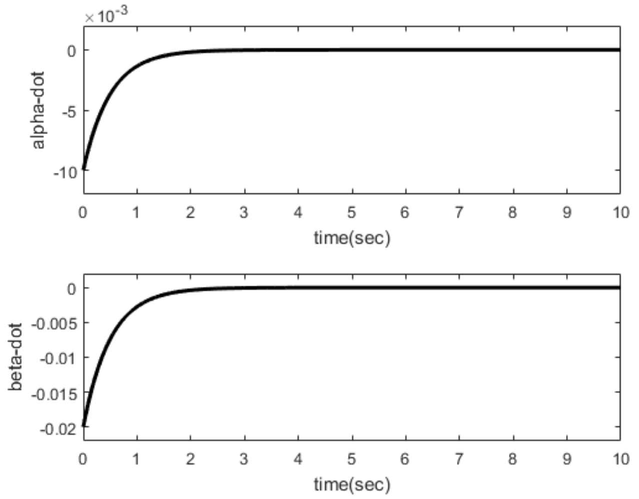

Fig. 13. The PBC-NC results for bicycle robot: the angle velocity of the steering angle and the angle velocity of the rolling angle with η =0.1

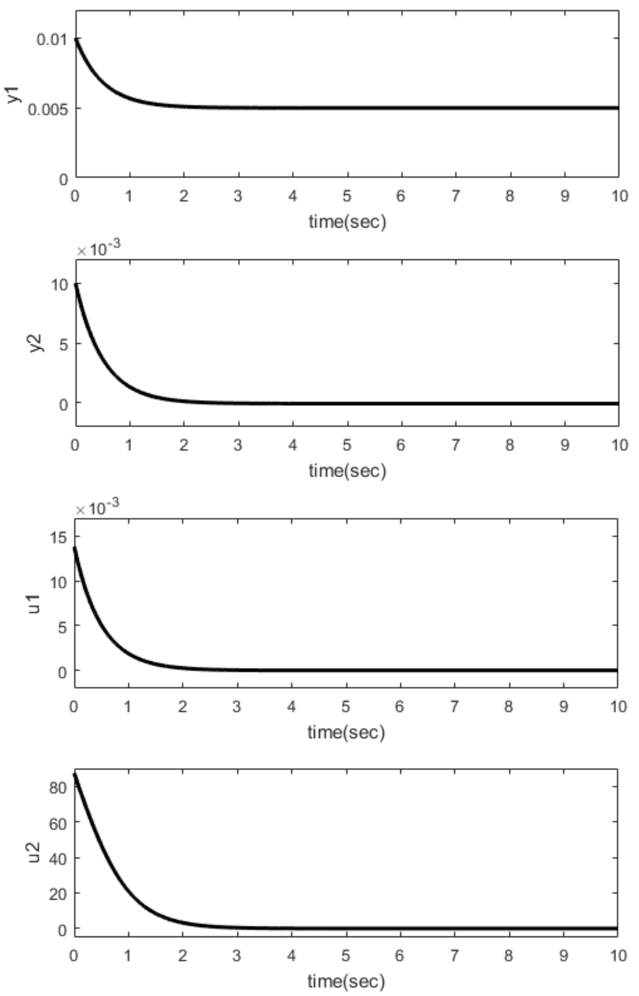

Fig. 14. The PBC-NC results for bicycle robot: the output signals y_1, y_2 and the control signal u_1, u_2 with η =0.1

V. CONCLUSION

In this paper, a comparative study of nonlinear control and passivity-based control using neural networks (PBC-NC) for a bicycle robot is proposed. The plant (7) is passive and the equilibrium point at origin is asymptotically stable. The variables $[x_1; x_2; x_3; x_4]$ and $[u_1; u_2]$ converge to [0; 0; 0; 0] and [0; 0] respectively. A training algorithm of neural network using the steepest descend method is proposed. Simulation results are done with Simulink in MATLAB. Simulation results show that the passivity-based control (PBC) and the passivity-based control using neural networks successfully maintain the vertical balance of the bicycle robot. However, the PBC-NC achieves a faster stabilization, with shorter settling times for both the steering angle and the rolling angle compared to the PBC. The settling time of the $\dot{\alpha}$ and the $\dot{\beta}$ of the PBC-NC is shorter than that of the PBC. Notably, when the learning constant η is increased, the PBC-NC shows further improvements in settling time, suggesting its superior performance over the traditional PBC in terms of responsiveness. The simulation results show that the settling time of the $\dot{\alpha}$ and the $\dot{\beta}$ of the passivity-based control using neural network is shorter when η is increased. The improvement in settling time when the learning constant is increased suggests that PBC-NC can adapt more efficiently to dynamic changes in the system, potentially leading to better real-time performance in real world applications. This makes PBC-NC an attractive option for enhancing the stability and responsiveness of robotic systems such as the bicycle robot. We compare the PBC-NC, with η =0.001, and the PBC-SMC of [37] which is applied to the bicycle robot. We can see that the PBC-SMC has shorter settling time than the PBC-NC with η =0.001. However, the output y_2 of PBC-SMC is equal to 0.005 (rad) and the output y_2 of PBC-NC is equal to 0 (rad). The results of this study contribute to the advancement of robotic control strategies by demonstrating the potential of neural network-based approaches in enhancing the performance of the passivity-based control systems. This work paves the way for more efficient algorithms that can be applied to other types of robotic systems requiring dynamic stability and balance control. Future work could explore the application of PBC-NC to more complex robotic systems and real-time environments, with an emphasis on overcoming computational limitations and ensuring robustness in the face of external disturbances. Additionally, the impact of different learning algorithms and parameter tuning on system performance could be investigated to optimize control strategies further.

Contributions of the Authors

Hoai Nghia Duong is the corresponding author. He guides the research idea, gives suggestion to the paper so that Minh Ngoc Huynh corrects the paper. He contributes the proposed training algorithm in section 3B. Vinh Hao Nguyen is the author. He guides the research idea, gives suggestion to the paper so that Minh Ngoc Huynh corrects the paper. Minh Ngoc Huynh is the first author. He writes the manuscript of the paper and does simulation. He corrects the paper according to Hoai Nghia Duong 's and Vinh Hao Nguyen 's suggestion, and the reviewer's comments. The authors all agree with the final manuscript to submit.

Acknowledgment

We acknowledge the support of time and facilities from Ho Chi Minh City University of Technology (HCMUT), VNU-HCM for this study.]

Abbreviations

PBC: passivity- based control.

NC: neural network control.

PBC-NC: passivity- based control using neural networks

PBC-SMC: passivity- based control – sliding mode control

SISO: single-input single-output.

MIMO: multi-input multi-output.

Declaration of Competing Interest

The authors declare that they have no known competing financial interests or personal relationships that could have appeared to influence the work reported in this paper.

References

[1] Y. Tanaka and T. Makami, "Self sustaining bicycle robot with steering controller," in *The 8th IEEE International workshop on Advanced motion control*, pp. 193-197, 2004, doi: 10.1109/AMC.2004.1297665.

[2] L. Guo, Q. Liao, S. Wei, and Y. Huang, "A kind of bicycle robot dynamic modeling and nonlinear control," in *The 2010 IEEE International Conference on Information and Automation*, pp. 1613-1617, 2010, doi: 10.1109/ICINFA.2010.5512251.

[3] K. J. Astrom, R. F. Klein, and A. Lennartsson. *Bicycle dynamics and control*. Lund University, Sweden, 2005.

[4] H. N. Duong. *Control of MIMO systems*. Ho Chi Minh City: VNU Press, 2013.

[5] H. K. Khalil. *Nonlinear systems*. New Jersey: Prentice-Hall 3rd edition, 2002.

[6] H. N. Duong and M. N. Huynh, "Control of bicycle robot using input-output linearization," *HCMUTE Journal of Technical Education Science*, vol. 15, no. 6, pp. 33-39, 2020.

[7] A. Turnwald, M. Schäfer and S. Liu, "Passivity-Based Trajectory Tracking Control for an Autonomous Bicycle," *IECON 2018 - 44th Annual Conference of the IEEE Industrial Electronics Society*, pp. 2607-2612, 2018, doi: 10.1109/IECON.2018.8591382.

[8] M. N. Huynh, H. N. Duong, and V. H. Nguyen, "Passivity-based control of bicycle robot," *VNUHCM Journal of Engineering and Technology*, vol. 5, no. 2, pp. 1520-1527, 2022, doi: 10.32508/stdjet.v5i2.954.

[9] L. Guo, H. Lin, J. Jiang, Y. Songi, and D. Gan, "Combined control algorithm based on synchronous reinforcement learning for a self-balancing bicycle robot," *ISA Transactions*, vol. 145, pp. 479-492, 2024, doi: 10.1016/j.isatra.2023.11.032.

[10] H. Zhao, W. Liu, X. Chen, and H. Sun, "Adaptive robust constraint – following control for underactuated unmanned bicycle robot with uncertainties," *ISA Transactions*, vol. 143, pp. 144-155, 2023, doi: 10.1016/j.isatra.2023.09.016.

[11] L. Chen, B. Yan, H. Wang, K Shao, E. Kurniawan, and G. Wang, "Extreme-learning-machine-based integral terminal sliding mode control of bicycle robot," *Control Engineering Practiice*, vol. 121, 2022, doi: 10.1016/j.conengprac.2022.105064.

[12] P. Seekhao, K. Tungpimolrut, and M. Parnichkun, "Development and control of a bicycle robot based on steering and pendulum balancing," *Mechatronics*, vol. 69, 2020, doi: 10.1016/j.mechatronics.2020.102386.

[13] L. Guo, Z. Chen, and Y. Song, "Semi-empirical dynamics modeling of a bicycle robot based on feature selection and RHONN," *Neurocomputing*, vol. 511, pp. 448-461, 2022, doi: 10.1016/j.neucom.2022.09.062

[14] D. Aschenbrenner, A. F. Burglund, M. Netten, Z. Rusak, and J. Stahre, "Sustainable human robot co-production for the bicycle industry," *Procedia CIRP*, vol. 104, pp. 857-862, 2021, doi: 10.1016/j.procir.2021.11.144.

[15] J. Baltes, G. Christmann, and S. Saeedvand, "A deep reinforcement learning algorithm to control a two-wheeled scooter with a humanoid robot," *Engineering Applications of Artificial Intelligence*, vol. 126, 2023, doi: 10.1016/j.engappai.2023.106941.

[16] R. Pieroni, M. Corno, F. Parravicini, and S. M. Savaresi, "Dsign of an automated street crossing management module for a delivery robot," *Control Engineering Practice*, vol. 153, 2024, doi: 10016/j.conengprac.2024.106095.

[17] M. Seder and G. Klancar, "Convergent wheeled robot navigation based on an interpolated potential function and gradient," *Robotics and Autonomous Systems*, vol. 177, 2024, doi: 10.1016/j.robot.2024.104712.

[18] F. Canadas-Aranega, J. C. Moreno, and J. L. Blanco-Claraco, "A PID-based control architecture for mobile robot path planning in greenhouses," *IFAC-PapersOnline*, vol. 58, no. 7, pp. 503-508, 2024, doi: 10.1016/j.ifacol.2024.08.112.

[19] Y. Zhang, G. Zhao, and H. Li, "Multibody dynamic modeling and controlling for unmanned bicycle system," *ISA Transactions*, vol. 118, pp. 174-188, 2021, doi: 10.1016/j.isatra.2021.02.014.

[20] M. Xia, A. Rahnama, S. Wang, and P. J. Antsaklis, "Control design using passivation for stability and performance*," IEEE Transactions on Automatic Control*, vol. 63, no. 9, pp. 2987-2993, 2018, doi: 10.1109/TAC.2018.2789681.

[21] T. S. Nguyen, N. H. Hoang, and M. A. Hussain, "A passivation approach to the control design of non-passive nonlinear system," *AJChE*, vol. 17, no. 2, pp. 86-105, 2017.

[22] M. Jankovic, D. Fontaine, and P. V. Kokotovic, "TORA Example: cascade and passivity-based control design," *IEEE Transactions on Control systems technology*, vol. 4, no. 3, pp. 292-297, 1996, doi: 10.1109/87.491203.

[23] M. Defoort and T. Murakami, "Second order sliding mode control with disturbance observer for bicycle stabilization," in *2008 IEEE/RSJ International Conference on Intelligent Robots and systems*, pp. 2822-2827, 2008, doi: 10.1109/IROS.2008.4650685.

[24] T. T. Bui, and M. Parnichkun, "Balancing control of bicyrobo by particle swarm optimization –based structure –specified mixed H_2/H_∞control," *International Journal of Advanced Robotic Systems*, vol. 5, pp. 395-402, 2008, doi: 10.5772/6235.

[25] X. Lin and X. Fang, "Passive backstepping control of dual active bridge converter in modular three-port converter," *Journal of Electronics, Basel*, vol. 12, no. 5, 2023, doi: 10.3390/electronics. 12051074.

[26] G. Q. B. Tran, P. Bernard, "Arbitrarily fast robust KKL observer for nonlinear time-varying discrete systems," *IEEE Transactions on Automatic control*, vol. 69, no. 3, pp. 1520-1535, 2024, doi: 10.1109/TAC.2023.3328833.

[27] M. Bin, P. Bernard, and L. Marconi, "Approximate nonlinear regulation via identification-based adaptive internal models," *IEEE Transactions on Automatic control*, vol. 66, no. 8, pp. 3534-3549, 2021, doi: 10.1109/TAC.2020.3020563.

[28] M. Li, G. Chesi, and Y. Hong, "Input-Feedforward-passivity-based distributed optimization over jointly connected balanced digraphs," *IEEE Transactions on Automatic Control*, vol. 66, no. 9, pp. 4117-4131, Sept. 2021, doi: 10.1109/TAC.2020.3028838.

[29] T. K. Nizami and A. Chakravarty, "Neural network integrated adaptive backstepping control of DC-DC boost converter," *Journal of IFAC-PapersOnline*, vol. 53, no. 1, pp. 549-554, 2020, doi: 10.1016/j.ifacol.2020.06.092.

[30] M. T. Vo, V. D. H. Nguyen, H. N. Duong, and V. H. Nguyen, "Combining passivity-based control and linear quadratic regulator to control a rotary inverted pendulum," *Journal of Robotics and Control (JRC)*, vol. 4, no. 4, 2023, doi: 10.18196/jrc.v4i4.18498.

[31] W. Liu, X. Cui, J. Zhou, Z. Zhang, M. Hou, S. Shan, and S. Wu, "Composite passivity based control of dc/dc boost converters with constant power loads in dc microgrid," *Journal of Power Electronics*, vol. 22, pp. 1927-1937, 2022, doi: 10.1007/s43236-022-00492-0.

[32] E. Rodriguez, R. Leyva, G.G. Farivar, H.D. Tafti, C.D. Townsend, and J. Pou, "Incremental passivity control in multilevel cascaded H-Bridge converters," *IEEE Transactions on Power electronics*, vol. 35, no. 8, pp. 8766-8778, August 2020, doi: 10.1109/TPEL.2020.2965164.

[33] V. Krishnamurthy and G. Yin, "Multikernel passive stochastic gradient algorithms and transfer learning," *IEEE Transactions on Automatic control*, vol. 67, no. 4, pp. 1792-1805, April 2022, doi: 10.1109/TAC.2021.3079280.

[34] A. Baraean, M. Kassas, M. S. Alam, and M. A. Abido, "Physics-informed NN-based adaptive backstepping terminal sliding mode control of buck converter for PEM electrolyzer," *Journal of Heliyon*, vol. 10, no. 7, April 2024, doi: 10.1016/j.heliyon.2024.e29254.

[35] R. Ortega, A. Loria, Per J. Nicklasson, and H. Sira-Ramirez. *Passivity-based control of Euler-Lagrange systems*. London: Springer-Verlag, 1998.

[36] M. N. Huynh, H. N. Duong, and V. H. Nguyen, "Passivity-based control using genetic algorithm for a dc-dc boost power converter," *VNUHCM Journal of Engineering and Technology*, vol. 6, no. 2, pp. 1891-1905, 2023, doi: 10.32508/stdjet.v6i2.1053.

[37] M. N. Huynh, H. N. Duong, and V. H. Nguyen, "A passivity-based control combined with sliding mode control for a dc-dc boost power converter," *Journal of Robotics and Control*, vol. 4, no. 6, pp. 780-790, 2023, doi: 10.18196/jrc.v4i6.20071.

[38] K. Shipra and R. Maurya, "Brayton-Moser passivity-based controller for an on-board integrated electric vehicle battery charger," *Journal of Energy Storage*, vol .75, 2024, doi: 10.1016/j.est.2023.109652.

[39] L. Martinez, D. Fernandez, and R. Mantz, "Passivity-based control for an isolated DC microgrid with hydrogen energy storage system," International Journal of Hydrogen energy, vol. 67, pp. 1262-1269, 2024, doi: 10.1016/j.ijhydene.2024.01.324

[40] N. Chopra, M. Fujjta, R. Ortega, and M. W. Spong, "Passivity-based control of robots: theory and examples from the literature," *IEEE Control Systems Magazine*, vol. 42, no. 2, pp. 63-72, 2022, doi: 10.1109/MCS.2021.3139722.

[41] H. Komurcugil, S. Bayhan, N. Guller, and R. Guzman, "Passivity-based control of four-switch buck-boost DC-DC converter without operation mode detection," in *IECON 2022- 48th Annual Conference of the IEEE Industrial Electronics society*, pp. 1-6, 2022, doi: 10.1109/IECON49645.2022.9968779.

[42] O. Penaloza-Mejia, Ojeda-Perez, and H. J. E. Garcia, "Passivity-based tracking control of robot manipulators with torque constraints," in *IEEE International Conference on Advanced Intelligent Mechatronics*, pp. 947-952, 2016, doi: 10.1109/AIM.2016.7576891.

[43] B. Said, T. Ilyes, K. Okba, D. E. Zabia, and M. Messaoud, "Optimized passivity-based control of a hybrid electric vehicle source using a novel optimizer," *Electrotehnika, Electronica, Automatica EEA; Bucharest*, vol. 71, no. 3, pp.23-31, 2023, doi: 10.46904/eea.23.71.3.1108003.

[44] J. Zhou, Q. Zhang, M.A. Hassan, Z. Zhana, M. Hou, S.Wu, Y. Li, E. Li, and J.M. Guerrero, "A robust passivity based model predictive control for buck converter suppling constant power load," *Energy Reports*, vol. 7, no. 7, pp.792-813, November 2021, doi: 10.1016/j.egyr.2021.09.193.

[45] Q. Xian, Y. Wang, F. Wang, R. Li, and S. Wang, "Hybrid passivity-based control for stability and robustness enhancement in dc microgrids with constant power loads," *Journal of Power Electronics*, vol. 23, pp. 296-307, 2023, doi: 10.1007/s43236-022-00529-4.

[46] C. Zhu, Y. Jiang, and C. Yang, "Fixed-time neural control of robot manipulator with global stability and guaranteed transient performance," *IEEE Transaactions on Industrial Electronics*, vol. 70, no. 1, pp. 803-812, 2023, doi: 10.1109/TIE.2022.3156037.

[47] M. Muthirayan and P. P. Khargonekar, "Memory augmented neural network adaptive controller: performance and stability," *IEEE Transactions on Automatic Control*, vol. 68, no. 2, pp. 825-838, 2023, doi: 10.1109/TAC.2022.3144382.

[48] Z. Zhai, H. Yan, S. Chen, X. Zhan, and H. Zeng, "Further results on dissipativity analysis for the T-S fuzzy systems based on sampled-data control," *IEEE Transactions on Fuzzy systems*, vol. 31, no.2, pp. 660-668, 2023, doi: 10.1109/TFUZZ.2022.3187177.

[49] Y. C. Chang and S. Gao, "Stabilizing neural control using self-learned almost Lyapunov critics," in *2021 IEEE International Conference on Robotics and Automation (ICRA)*, pp. 1803-1809, 2021, doi: 10.1109/ICRA48506.2021.9560886.

[50] Q. Xiao, T. Huang, and M.A. Hussain, "Passivity and passification of fuzzy memristive inertial neural networks on time scales," *IEEE Transactions on Fuzzy systems*, vol. 26, no. 6, pp. 3342-3355, December 2018, doi: 10.1109/TFUZZ.2018.2825306.

[51] J. Qiu, W. Ji, and M. Chadli, "A novel fuzzy output feedback dynamic siding mode controller design for two-dimensional nonlinear systems," *IEEE Transaction on Fuzzy systems*, vol. 29, no. 10, pp. 2869-2877, October 2021, doi: 10.1109/TFUZZ.2020.3008271.

[52] M. C. Huynh and C. Y. Chang, "A novel adaptive neural controller for narrowband active noise control systems," in *2021 8th NAFOSTED*

Conference on Information and Computer Science (NICS), pp. 504-506, 2021, doi: 10.1109/NICS54270.2021.9701565.

[53] F. Shen, X. Wang, and X. Yin, "BLF-based adaptive DSC for a class of stochastic nonlinear systems of full state constraints with time delay and hysteresis input," *Journal of Neurocomputing*, vol. 386, pp. 244-256, April 2020, doi: 10.1016/j.neucom.2019.12.102.

[54] M. Rahmani and S. Redkar, "Deep neural data-driven Koopman fractional control of a worm robot," *Journal of Expert systems with applications*, vol. 256, 2024, doi: 10.1016/j.eswa.2024.124916.

[55] X. Li, X. Ren, Z. Zhang, J. Guo, Y. Luo, J Mai, and B. Liao, "A varying parameter complementary neural network for multi-robot tracking and formation via model predictive control," *Journal of Neurocomputing*, vol. 609, 2024, doi: 10.1016/j.neucom.2024.128384.

[56] A. Tsiamis and G. J. Pappas, "Online learning of the Kalman Filter with the logarithmic regret," *IEEE Transactions on Automatic Control*, vol. 68, no. 5, pp. 2774-2789, 2023, doi: 10.1109/TAC.2022.3207670.

[57] R. D. McAllister and J. B. Rawlings, "Inherent stochastic robustness of model predictive control to large and infrequent disturbances," *IEEE Transactions on Automatic Control*, vol. 67, no. 10, pp. 5166-5178, 2022, doi: 10.1109/TAC.2021.3122365.

[58] S. He, C. Zou, Z. Deng, W. Liu, B. He, and J. Zhang, "Model-less optimal visual control of tendon-driven continuum robots using recurrent neural network-based neurodynamic optimization," *Robotics and Autonomous systems*, vol. 182, 2024, doi: 10.1016/j.robot.2024.104811.

[59] Y. Zhang, Z. Xu, J. Chen, L. Zhao, X. Wang, and C. Hua, "Neural networks-based composite learning control for robotic systems with predefined time error constraints," *Journal of Neurocomputing*, vol. 608, 2024, doi: 10.1016/j.neucom.2024.128414.

[60] T. Gao, "Optimizing robotic arm control using deep Q-learning and artificial neural networks through demonstration –based methodologies: A case study of dynamic and static conditions," *Robotics and Autonomous systems*, vol. 181, 2024, doi: 10.1016/j.robot.2024.104771.

[61] M. B. Suarez *et al*., "A robust two-stage active disturbance rejection control for the stabilization of a riderless bicycle," *Journal of Multibody System Dynamics*, vol. 45, pp. 7-35, 2019, doi: 10.1007/s11044-018-9614-y.

[62] J. Son, H. Kang, S. H. Kang, "A review on robust control of robot manipulators for future manufacturing," *International Journal of Precision Engineering and Manufacturing*, vol. 24, pp. 1083-1102, 2023, doi: 10.1007/s12541-023-00812-9.

[63] M. T. Vo, H. N. Duong, and V. H. Nguyen, "Comparative study of swing-up controllers: passivity-based swing-up control and sliding mode technique combined energy-based method for rotational inverted pendulum system," in *2024 9th International Conference on Applying new technology in green buildings (AtiGB)*, pp. 218-223, August 2024, doi: 10.1109/ATiGB63471.2024.10717747.

[64] N. T. Tran, M. H. Tran, T. N. P. Nguyen, and D. T. Tran, "Modelling and experimental analysis for a two legged wheel robot with a fuzzy lqr control," in *2024 7th International Conference on Green technology and sustainable development (GTSDD)*, pp. 340-344, July 2024, doi: 10.1109/GTSD62346.2024.10674859.

[65] A. Garus, P. Christidis, A. Mourtzouchou, L. Dubos, and B. Ciuffo, "Unravelling the last-mile conundrum: a comparative study of autonomous delivery robots, delivery bicycles, and light commercial vehicles in 14 varied European landscapes," *Sustainable cities and society*, vol. 108, August 2024, doi: 10.1016/j.scs.2024.105490.

[66] A. Top and M. Gokbulut, "Real-time deep learning-based position control of a mobile robot," *Engineering Applications of Artificial Intelligence*, vol. 138, 2024, doi: 10.1016/j.engappai.2024.109373.

[67] M. Norgaard *et al*., *Neural networks for modelling and control of dynamic systems*. Berlin: Springer, 1st edition, 2000.

[68] C. Ehrmann, J. Min, and W. Zhong, "Highly flexible robotic manufacturing cell based on holistic real-time model-based control," *Procedia CIRP*, vol. 127, pp. 20-25, 2024, doi: 10.1016/j.procir.2024.07.005.

[69] Z. Liu, J. Yu, and H. K. Lam, "Passivity-based adaptive fuzzy control for stochastic nonlinear switched systems via T-S fuzzy modeling," *IEEE Transactions on Fuzzy Systems*, vol. 31, no. 4, pp. 1401-1408, April 2023, doi: 10.1109/TFUZZ.2022.3195645.

[70] S. Liu, H. Zhang, and H. Pang, "Semipassivity-based fuzzy tracking control for switched nonlinear systems," *IEEE Transactions on Fuzzy Systems*, vol. 32, no. 1, pp. 126-136, January 2024, doi: 10.1109/TFUZZ.2023.3292316.

[71] X. Wang, B. Niu, X. Zhao, G. Zong, T. Chen, and B. Li, "Command-filtered adaptive fuzzy finite-time tracking control algorithm for flexible robotic manipulator: a singularity-free approach," *IEEE Transactions on Fuzzy Systems*, vol. 32, no. 2, pp. 409-419, February 2024, doi: 10.1109/TFUZZ.2023.3298367.

[72] Y. Wang and W. Lin, "Input delay tolerance of nonlinear systems under smooth feedback: a semiglobal control framework," *IEEE Transactions on Automatic control*, vol. 67, no. 1, pp. 146-161, January 2022, doi: 10.1109/TAC.2020.3046709.

[73] C. Y. Ciao, R. G. Chang, and H. C. Huang, "Robotic arms for telemedicine system using smart sensors and ultrasound robots," *Internet of Things*, vol. 27, October 2024, doi: 10.1016/j.iot.2024.101243.

[74] I. A. Kuncara, A. Wydiotriatmo, A. Hasan, and Y. Y. Nazaruddin, "Enhancing accuracy in field mobile robot state estimation with GNSS and encoders," *Measurements*, vol. 235, August 2024, doi: 10.1016/j.measuremment.2024.114903.

[75] O. Uyar, M. Kuncas, and H. Karaca, "Enhanced intelligent control with adaptive system for electrically assisted bicycle," *Engineering Science and Technology, an International Journal*, vol. 30, June 2022, doi: 10.1016/j.jestch.2021.08.004.

[76] M. Efken, M. Kohn, D. Kreven, and B. J. E. Misgeld, "Cooperative control of electrical bicycles," *IFAC Journal of Systems and Control*, vol. 16, June 2021, doi: 10.1016/j.ifacsc.2021.100153.

[77] N. C. Sanchez, I. Martinez, L. A. Pastor, and K. Larson, "On the performance of shared autonomous bicycles: a simulation study," *Communications in Transportation Research*, vol. 2, December 2022, doi: 10.1016/j.commtr.2022.100066.

[78] H. Wu, D. Xu, and B. Jayawardhana, "On self-learning mechanism for the output regulation of second-order affine nonlinear systems," *IEEE Transactions on Automatic control*, vol. 67, no. 11, pp. 5964-5979, November 2022, doi: 10.1109/TAC.2020.3130881.